Rare Metal Materials and Engineering
Volume 48, Issue 6, June 2019
Available online at www.rmme.ac.cn

Science Press

Cite this article as: Rare Metal Materials and Engineering, 2019, 48(6): 1717-1724.

ARTICLE

Two-Layer Process and Optimal Blank Design for Hollow Titanium Wide-Chord Fan Blades with Complex Geometries

Chen Minghe, Wu Xinchen, Xie Lansheng, Wang Ning, Su Nan

Nanjing University of Aeronautics and Astronautics, Nanjing 210016, China

Abstract: A new two-layer process based on hot forming and diffusion bonding for forming a hollow titanium wide-chord fan blade with complex geometries was developed. An essential approach for optimal blank design was proposed. The present process employed a more reliable and controllable method to construct the internal ribbons, instead of complicated superplastic forming. To evaluate the practicability, a numerical method was used to investigate the thickness uniformity, structural integrity and skin defects of forming results using ABAQUS. A series of experiments were conducted to validate the simulation results. The Ti-6Al-4V alloy was adopted as the forming material, and blanks optimized by the proposed approach were used. The results show that a scaled-down version of the hollow wide-chord fan blade without defects is successfully formed. In addition, it is observed that the experimentation and simulation agree well.

Key words: hollow wide-chord fan blade; optimal blank design; diffusion bonding; finite element simulation; titanium alloy

Turbofan is widely used to provide highly efficient propulsion for aircraft, both in commercial and military aviation. As an important component of it, the fan blade is responsible for accelerating bypass flow and producing majority of the thrust; its structure and properties are closely associated with the engine's noise level, thrust-weight ratio, fuel efficiency, reliability, lifetime etc. Traditional titanium fan blades are characterized by narrow-chord design and solid construction[1]. For current turbofan applications, their inherent weight penalty sets an obstacle to the diameter enlargement and related bypass ratio promotion. Hence, the outdated ones were replaced by the advanced hollow titanium wide chord fan blade (WCFB), which shows obvious advantages in weight reduction. It has been widely used in modern engine types. However, the precise aero dynamic surface along with the sophisticated hollow structure makes the manufacturing practice very difficult. Further, the titanium alloy is generally considered to be hard to deform due to its higher yield ratio, lower elastic modulus, and worse plasticity at room temperature. Almost all the hollow metal fan blades are manufactured by diffusion bonding (DB) combined with superplastic forming (SPF) or hot forming. So far, there are several methods about the fabrication of the hollow titanium fan blade, such as the honeycomb core, no core (two-layer), three-layer and four-layer sandwich processes.

Many researches published in recent years are focused on the fabrication of multi-sheet sandwich structures. Xun and Tan[2] fabricated a four-layer hollow Ti-6Al-4V engine blade with sandwich structure based on the SPF/DB process. Microstructures before and after thermal cycles were compared to analyze the grain growth; tensile tests were conducted to investigate the reduction in mechanical properties. Han et al[3] produced a four-layer honey-comb titanium structure using Ti-6Al-4V alloy through the SPF/DB process, and also Du et al[4] fabricated the same structure using Ti2AlNb alloy. Their research focused mainly on the effect of diffusion bonding parameters on shear strength of the joints. The microstructure and the thickness distribution were also investigated. It was confirmed that grain size of the material became larger, which can be attributed to superplastic deformation and the thermal exposure. Obviously, the thickness of sheet may have a large deviation during the procedure of three-layer or four-layer

Received date: June 12, 2019
Foundation item: Science and Technology Support Program of Jiangsu Province (BE2013123)
Corresponding author: Chen Minghe, Ph. D., Professor, College of Mechanical and Electrical Engineering, Nanjing University of Aeronautics and Astronautics, Nanjing 210016, P. R. China, E-mail: meemhchen@nuaa.edu.cn

processes. Huang et al[5] focused on the thinning control of sheet in the SPF process. In the numerical simulation and experiment, local thinning has been observed in the formed shape with constant initial sheet thickness. By using the modified sheet thickness profile that they proposed to achieve proportional control, a dome-shaped model with constant thickness has been successfully obtained with the maximum error reduced to 9%. Zhang et al[6] under- took three methods to control the thickness deviation in super- plastic forming, including superplastic forming accompanied by compression in the axial direction, superplastic direct and reverse bulging, and moving die superplastic forming. Certain degree of thickness variation has been seen in the final forming result. More than that, process control for the multi-sheet SPF/DB forming processes is quite complicated. Inappropriate parameters can easily lead to obvious sink mark on the structure skin in these processes. Yoon et al[7] employed the finite element analysis to investigate the factor for the defect in the four-layer structure. It was confirmed that the maximum forming pressure, forming time and optimal strain rate have significant effects on the formation of defects. Zhao et al[8] pointed out that the sheet thickness ratio of core sheet to face sheet along with other parameters such as the twisting rate, descending velocity, strain rate have an important influence on the forming result of the hollow blade. The existing three-layer or four-layer processes put forward high requirement on the process design and equipment fabrication.

As an alternative, the two-layer process provides a much more simplified and defection-free way for producing the hollow titanium fan blade. Unlike the multi-layer sandwich processes that use gas inflation to form the ribbons, this process employs a couple of pre-milled blanks with a in-process shape, which greatly reduces the manufacture complexity and facilitates the quality control. However, few researches have been published on it. In this paper, a two-layer process for fabricating hollow titanium wide chord fan blade was proposed with the supporting approach for blank design. Numerical and experimental methods were employed to evaluate the technical feasibility. The skin thickness uniformity, wall structural integrity and forming defects were investigated. The scaled-down version of the hollow wide-chord fan blade was successfully formed to prove the validation of this process.

1 Principle of the Proposed Two-Layer Process

The scaled-down sample of the hollow wide-chord fan blade used here for validating the process is demonstrated in Fig.1. The blade is about 215 mm in height and 245 mm in width. It is made of Ti-6Al-4V titanium alloy. Inside the entity, hollow structure occupies the majority of the foil, which comprises a plurality of cavities and ribs. The cavities relieve the considerable weight of the base while ribbons reinforce the outer skin, and the thickness of ribbons is 2 mm. In addition,

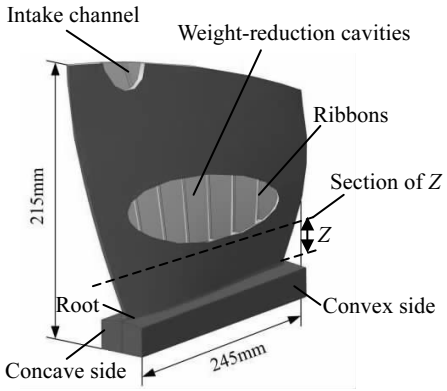

Fig.1 Demonstration of the hollow titanium wide chord fan blade

to enable the gas inflation, cavities are connected by small openings on the ribbons, and an intake channel is designed to penetrate into the cavity. The peripheral area of the foil and the tenon part remain solid to retain enough strength. The configuration of the blade presents various thicknesses and curvatures at different locations, while the thickness of the skin is uniformly 1.5 mm throughout the whole hollow area.

Fig.2 demonstrates the two-layer process proposed in this paper. The whole forming process involves four steps: diffusion bonding, heat twisting, mold pressing and inflation adjusting. To be detailed, this process employs a couple of semi-shape blanks. The outer has optimized in-process shape, and the cavities and ribbons are milled inside. The couple is assembled and placed in the diffusion bonding mold. Under the condition of diffusion temperature and appropriate bonding pressure, the interfaces of the couple begin to merge; void between them keeps shrinking due to the active atom diffusion. After a certain amount of time, the couple is bonded together into a single hollow blank. Then the hollow blank is twisted at a relatively low temperature to obtain an intermediate shape. The twisting tool is composed of a fixed clamp and a rotatable sleeve. The mold pressing serves as the following step to adjust the external shape of the twisted blade, relieving the differences between the actual profile and the nominal. In order to repair the skin defects emerging in the preceding steps, the inflation adjusting step is arranged finally. Under the control of a digital pressure controller, the argon is inflated into the blade cavities to blow the sunken skin up and to

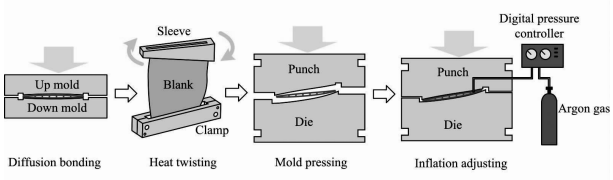

Fig.2 Manufacturing process for two-layer hollow titanium fan blades

smooth the grooves. After that, only polishing is needed to improve the surface rough degree.

This process is a kind of near net-shape manufacturing process with a relatively high material utilization rate. During this process, the most critical part is the specification of the blank shape. Due to the lower stiffness of the hollow region, the blank after bonding is unsuitable for a large amount of machining. The bonded couple is twisted and formed directly into the desired shape by mold pressing. Although the final shape obtained is determined by the mold, the initial shape is equally important to this process. On the one hand, if the blank has insufficient material stock, the formed blade will inevitably be locally too thin. The final shape will deviate from the desired profile. On the other hand, if the blank is over-dimensioned, the flow of excessive material will distort the ribs and lead to instability on the skin. Therefore, it puts forward high requirement on the accuracy of geometry and dimensional specification of blank. The error must be controlled within a limited range.

2 Experiment

2.1 Optimal blank design and diffusion bonding

Due to the nonlinear characters of material flow behavior and complex component geometry, it is hard to research the forming regularity theoretically and optimize the blank shape empirically. Traditional try-mold procedure is very costly and time consuming, which can hardly satisfy the demand. Based on the finite element method which is widely used to assist the process design nowadays, many optimal blank design methods are proposed. Lee and Huh[9] introduced an inverse approach for the prediction of blank shapes of the desired sheet metal part. Parsa et al[10] used the slip line field to improve the initial blank shape of the intricate products. However, these methods are just applied to sheet metal with a constant thickness. Feng et al[11] developed a large and thick shape of a Francis turbine blade for a hydropower plant by an inverse FE model. Nevertheless, his initial shape is uniform in thickness.

The blade in this paper is a solid component characterized by complex shape with varying thicknesses. The outside shape keeps changing during the deformation. The blank specification method should be emphasized on the thickness redistribution. Existing researches are mainly focused on the unfolding of sheet metal structures with uniform thickness, which are not applicable here. An approach based on the finite element method is proposed to specify the optimal blank shape for those components with unequal thickness. The essence of the approach is to flatten the mid-surface and deform the blade entity. It is realized by locating nodes on the neutral layer and forcing them to move to the needed plane by applying force, as shown in Fig.3. Driven by the flatting deformation of the mid-surface, the entire component deforms spontaneously due to the continuity of the material. When all the nodes of the mid-surface are right on the target plane, the mid-surface is

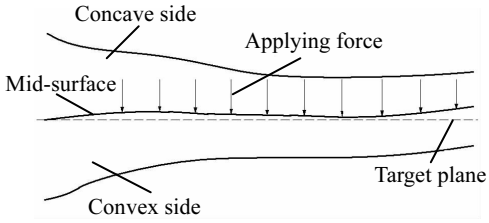

Fig.3 Description of the flatting approach

flat and the desired flat blank shape is obtained. During the deformation, the component is considered as solid and meshed by 3D elements with volume, instead of being abstracted into a shell with constant thickness, as described in the current methods. The approach takes the deformation compatibility into consideration and reproduces the actual material flow. More importantly, the flatting process is thoroughly internal driven without any forces or interactions exerted on the skin, which protects the external aerodynamic shape from innocent damage.

Some assumptions and simplifications were made in the approach. Firstly, influences of neutral layer movement are ignored. It is assumed that the position of the neutral surface remains static because the total thickness is relatively small. Secondly, the internal hollow structure is neglected during the flatting. The hollow foil is replaced by a corresponding solid one with a duplicate configuration.

The temperature rising procedure was controlled by a programmable digital controller. Temperature on the furnace wall was used as the feedback for the control system, and temperature of the mold was directly shown on the controller screen with the help of several thermocouples in the furnace. Due to the thermal inertia of the mold, the heating program was divided into several sections; each section comprises a temperature rising stage and an uniformization stage. It took 8.5 h for the mold temperature to reach the diffusion bonding temperature of 930 °C. According to the blade dimension, the applied force was controlled to generate a pressure of 3 MPa on the diffusion bonding interface. The bonding process took 1 h, during which the temperature was kept as stationary as possible. Then the heating was stopped, and load was relieved. During the furnace cooling period, the vacuum was remained to resist the oxidation and hydrogen absorption. It took about 15 h for the furnace to cool down.

2.2 Heat twisting

The process was conducted in a dedicated heat twisting apparatus. It is acted by a couple of vertical shafts with the freedom of up-down movement and rotation, which are driven by servo motors independently. According to the blade shape, a clamp and a sleeve were designed and fabricated using the 310S stainless steel. They were precisely installed on the shafts. The bonded blank was placed in the apparatus as its tenon was fixed by the clamp and its tip was fitted in the

sleeve. Its outer surface was coated by a thick layer of boron nitride powder as a protection. Prior to heating, alternating rounds of air extraction and argon gas inflation were performed to reduce the oxygen concentration in the furnace chamber. During the heating, the pressure of the argon inside the furnace chamber was maintained slightly higher than the local atmospheric pressure. As no mold is included, the thermal inertia is quite small and thus the heating speed can be promoted. It took 1 h for the furnace temperature to rise to 750 °C and another 40 min was used to make the temperature uniform. Then the twisting began. Within 30 min, the clamp kept static and the sleeve rotated 20.4° at a uniform speed. Finally, it took about 12 h for the furnace to cool down in the argon atmosphere.

2.3 Mold pressing and inflation adjusting

In order to correct the blade configuration and repair the skin defection, the mold pressing and inflation adjusting procedure were arranged after twisting. A nodular iron with molybdenum and moderate silicon was used to produce the pressing mold. Based on the final shape of the blade, the pressing mold was designed. The mold cavity was scaled down to compensate the differentials in the thermal expansion coefficient between different materials. The punch and die were mounted on the heating platforms with 1500 kN heat press. A pipe of Ti-6Al-4V with 8 mm in outside diameter and 1 mm in thickness was connected with the intake channel to inflate gas inside the blade cavities and to blow the grooved skin up. It is bonded to the blade entity by argon arc welding. In addition, a section of stain steel 304 pipe was used to wrap the titanium pipe to prevent its excessive creep deformation, as shown in Fig.4. Due to the absence of argon atmosphere and vacuum environment, the oxidation tends to be serious during the heating. The mold and blade were coated with a thick layer of boron nitride powder, and the pipe was coated with colloidal graphite powder. Before heating, several rounds of air extraction and argon inflation were performed to reduce the oxygen concentration in the blade cavities.

It took 10 and 5 h for the mold to reach the forming temperature of 750 °C and thermos uniformization, respectively. The punch speed was set to be 0.4 mm/s, which is close to the minimum limit of the press. As the punch moved downward, the blade profile was rectified. After the mold closed completely, the keeping pressure of the main cylinder was set to be 4 MPa. Then argon gas was inflated into the hollow structure through the pipe. The inflation pressure was controlled by a programmable closed-loop pressure control system. In this process, the pressure cycle was considerably simplified compared to the existing multi-layer craft. Here a regular pressure curve was used, as shown in Fig.5.

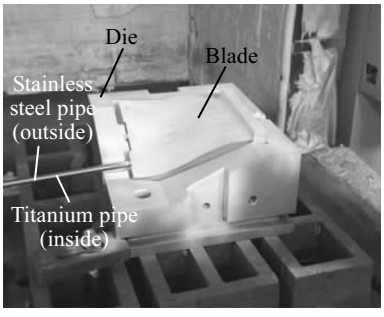

Fig.4 Intake pipe installation and die mounting

3 Result and Discussion

3.1 Result of flatting operation

In the first step, the blade was twisted backwards into a near blank shape by applying torque. Fig.6a illustrates the velocity vectors of nodes on the mid-surface in a moment of this course. It can be seen that all nodes move toward the flatted plane at different speeds along different orientations. The obtained mesh at the end of the first step is shown in Fig.6b. It can be seen that most regions of the blade are flatted preliminarily. And also the regions near the trailing edge and the root remain curved and need to be further flatted.

With the couple of rigid faces pressing nodes of the neutral surface from both sides in the second step, the blade was completely flatted into the blank shape. Fig.7a shows velocity vectors of nodes on the mid-surface in this step. Nodes on the

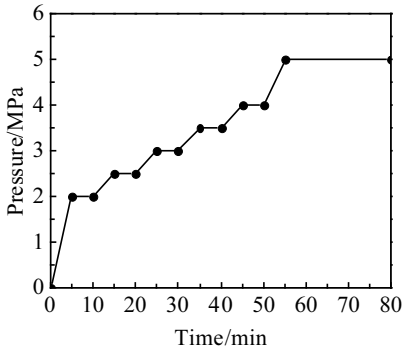

Fig.5 Pressure cycle of the inflation adjusting

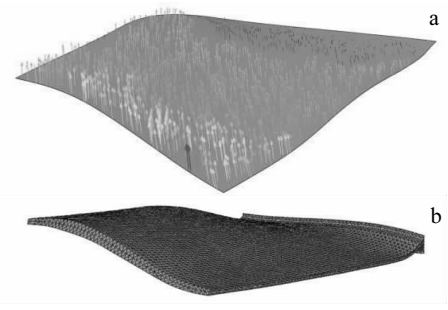

Fig.6 Blade twisted backwards: (a) velocity vectors of nodes on the mid-surface and (b) mesh obtained by the first step

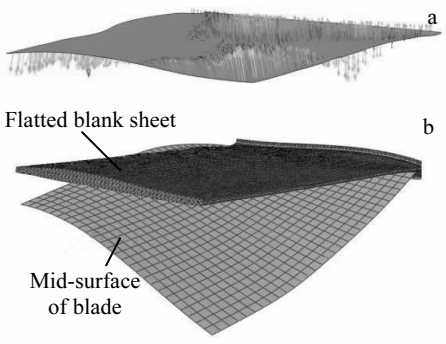

Fig.7 Comparison between the obtained blank and the middle surface of original blade: (a) velocity vectors of nodes on the mid-surface and (b) mesh obtained by the second step

mid-surface taking the final step move to the target plane following different paths. Compared with the middle surface of the initial blade, the flatted mesh obtained by the second step is shown in Fig.7b. It is observed that the method apparently works and the flatting effect is remarkable.

Fig.8 illustrates the plane strain of the neutral surface after flatting. It can be seen that in most regions, the strain is small enough to assume that no elongation occurs on it. However, in regions with initial bending deformations (region Ⅰ), apparent strains are observed. The leading edge (region Ⅱ) and trailing edge (region Ⅳ) with initial curvature also present a certain amount of strain. The presented strain on the neutral surface is considered as the result of the movement of mid-surface during bending deformation as it tends to move towards the center of the curve. While on the other area where the deformation is moderate (region Ⅲ), the mid-surface remains unmoved and thus strain can be hardly observed.

In order to research the thickness redistribution after flatting, three representative vertical-sections A-A, B-B, C-C (Fig.9) were selected and the thickness change compared to their original shape is illustrated in Fig.10. The section A-A is located near the leading edge which has concentrated bending deformation. The section B-B is located in the middle of the blade, on which the curvature is small and the blade root remains perpendicular to the tenon. The section C-C is located near the leading edge and there is repeated bending on it. In each section, thicknesses were measured by inquiring the

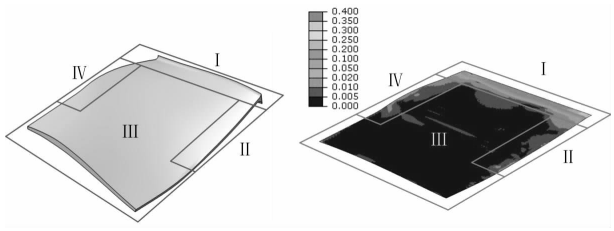

Fig.8 Strain distribution on the neutral surface

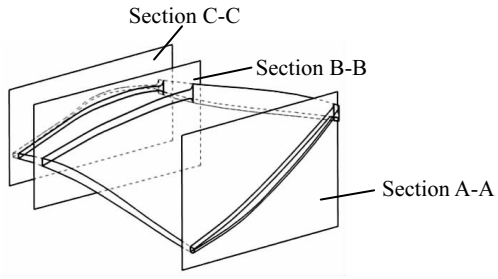

Fig.9 Section definition

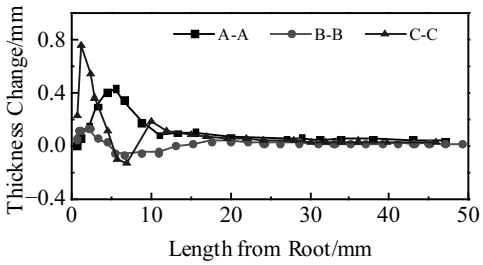

Fig.10 Thickness distribution of section A-A, B-B and C-C

distance between the corresponding nodes on the convex skin and the concave skin before and after flatting. It can be seen that: (1) thicknesses in the blade root increases to various degrees due to the material flowing. The increment increases with initial deformation, as the growth of section C-C and A-A is apparently more than that of section B-B in the same location; (2) each thickness growth is accompanied by a certain degree of thickness decrease, obeying the constant-volume principle. Volume increase in one region will inevitably be complemented by surrounding material, resulting in a decrease in thickness; (3) thickness of regions outside the root area (length more than 20 mm from the root) with moderate initial deformation remains fairly unchanged. The configuration of the blank totally changes after flatting due to the complex material flow and deformation compatibility.

3.2 Twisting result

The deformed mesh after twisting is shown on the left side of Fig.11, and the blank obtained by experiment is shown on the right side as a comparison. It is obvious that the blank is formed into a warped shape with the whole foil leaning against one side. The twisting simulation shows great agreement with the experimental result and predicts the deformation precisely as the deformed grid shape closes the obtained twisted blade. This shape serves as an ideal intermediate between the initial blank and the final complex distorted configuration. It fits the pressing mold better and can be placed in it much more easily. However, it can be seen that some grooves appear on the skin of the blades.

Fig.12 shows the FEM results of strain distribution after twisting. It can be found that most of the strain is distributed

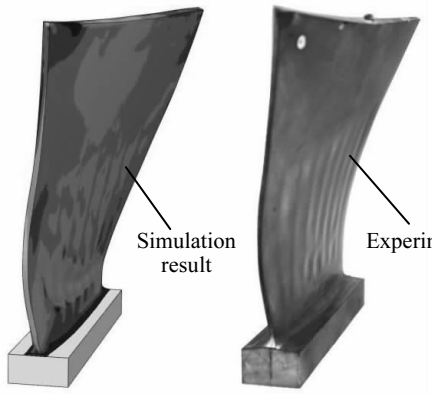

Fig.11 Twisted hollow blank at a twist angle of 20.4° and a temperature of 750 °C

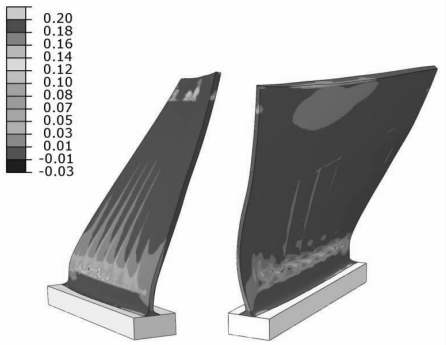

Fig.12 Strain distribution after twisting at a twist angle of 20.4° and a temperature of 750 °C

near the heel of the blade. The maximum tensile strain is located at the border between the solid and the hollow regions. Across the border, the distribution and magnitude of strain are quite different, especially on the hollow side. However, within the root region, the strain is very limited. The possible reason is that the stiffness of the root is too huge to bend and twist, and deformation is transferred to the hollow region with relatively small deformation resistance. Besides, the groove region on the skin shows an extremely large strain exceeding 0.2.

The FEM simulation predicts the occurrence of grooves on the skin near the root region after twisting, which was verified by the experiment result. It indicates that instability takes place, which is closely related to the local stress state. The hollow cavities are covered by the skin with a uniform thickness of 1.5 mm, which can be considered as a blank sheet with initial curvature. The load applied by the sleeve can be simplified to a concentrated force F and moment T. An element in the surface deflection is taken out for discussion, as shown in Fig.13. The element stands the compressive stress σ_1 along the length direction induced by the bending effect of force F and the compressive stress σ_2 induced by the torsional shear effect of moment T. Thus, material in this region is

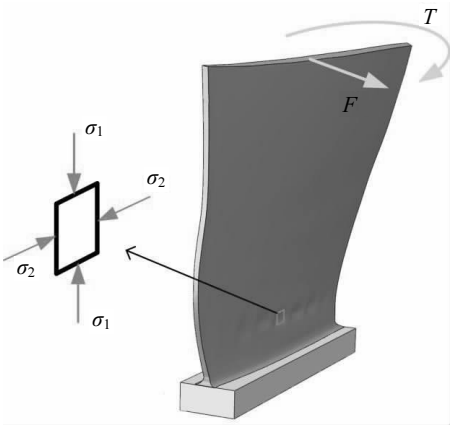

Fig.13 Stress analysis of the groove region

under the biaxial compressive loading and is easily subjected to compress instability. The distribution of stresses along direction X and Z is shown in Fig.14. It can be seen that when the sleeve rotates by 9.2°, the region where surface deflection occurs has a significant tendency of compressive stress concentration, which directly leads to the instability.

3.3 Result of mold adjusting

The deformed grid was used as the initial mesh in the pressing and inflating simulation, as shown in Fig.15a. As the distance between punch and die keeps narrowing, the blade begins to interact with the mold and continues to deform in it. The finished shape after pressing is shown in Fig.15b. It can

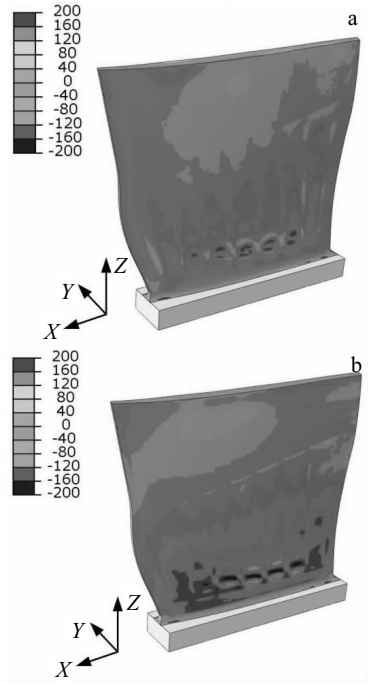

Fig.14 Stress distribution at a twist angle of 20.4° and a temperature of 750 °C: (a) X-stress (MPa) and (b) Z-stress (MPa)

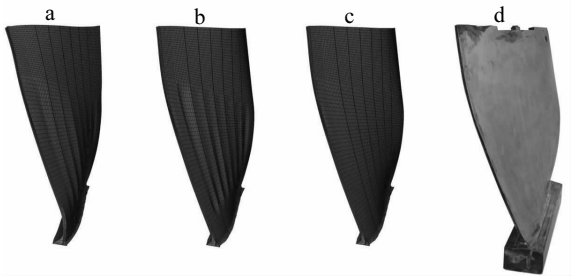

Fig.15 Deformed mesh (a) and finished component (b) at 750 °C; applying uniform pressure on the inner face of the hollow structure (c) and sample piece obtained by experiments (d)

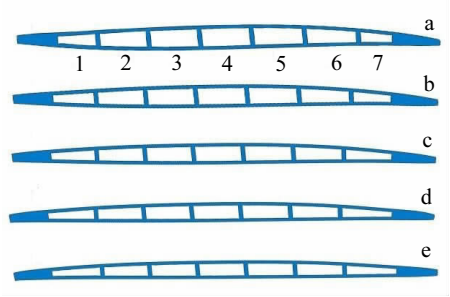

Fig.17 Sections of the hollow region: (a) *Z*=25 mm, (b) *Z*=40 mm, (c) *Z*=60 mm, (d) *Z*=80 mm, and (e) *Z*=100 mm

be seen that the root region is formed into the desired shape. Nonetheless, the grooves remain on the skin. For repairing the defective area, argon was inflated into the internal cavities. This process was simulated by applying uniform pressure on the inner face of the hollow structure, and the result is shown in Fig.15c. The sample piece obtained by experiments is shown in Fig.15d. It is clear that the results of simulation and experimental agree well, indicating that the FEM model can be used to simulate this process.

Fig.16 shows the strain distribution of the finished blade after mold adjusting. It can be found that the maximum strain is located near the blade root within a relatively tenuous area. Besides this area, the strain distribution in the remaining area is much more equal, indicating that the deformation is spread throughout the whole region.

As the internal ribbons are used to provide reinforcement on the skins, their figures must be kept upright. Fig.17 shows several sections in the hollow region of the FEM result after the inflation adjusting. *Z* and its section are defined in Fig.1. It can be seen that the distortion of the ribbons is controlled within a small range. Most ribbons maintain their initial shape without apparent buckling. It can be concluded that the blank sheet is well dimensioned and the structural integrity after forming can meet the requirement.

In each section, the thicknesses of convex and concave skins in formed mesh are plotted in Fig.18 and Fig.19, respectively. Compared with the initial thickness of 1.5 mm, skin thicknesses of hollow region generally increase by about 3.3%~6.7%. The midpoint of the cavity 7 skin on the section of *Z*=25 mm is the thickest point throughout the convex skin with a thickness of 1.605 mm and a growth of 7%. Similarly, the counterpart on the concave skin is the thickest point with a thickness of 1.615 mm and a growth of 7.6%. In general, the skin thickness growth shows an increasing tendency from the leading edge to trailing edge in both convex and concave sides. The thickness on the section nearest to the root shows the largest increment compared to other sections, which can be attributed to the complex material flow.

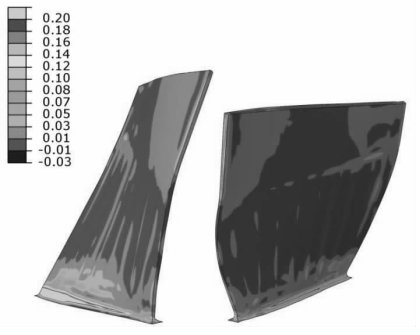

Fig.16 Strain distribution after inflation at maximum pressure of 5 MPa (750 °C)

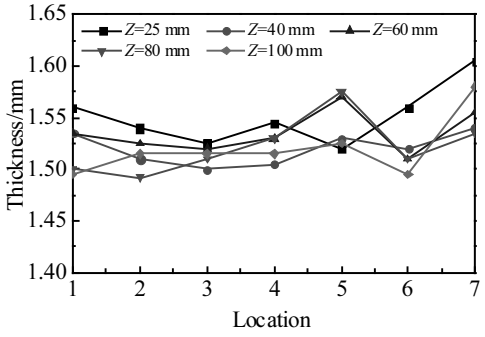

Fig.18 Thickness of the convex skin

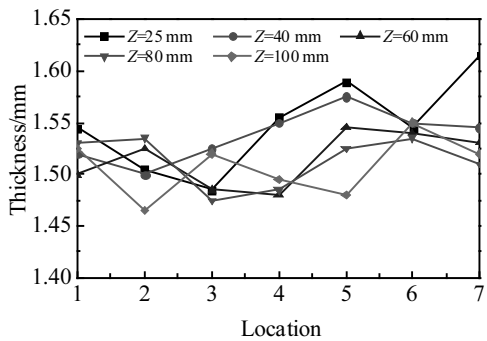

Fig.19 Thickness of the concave skin

4 Conclusions

1) The blank shape obtained by the proposed approach is quite applicable for the process, and no apparent volume void or over-dimension is observed. Due to the complexity of geometries, complicated material flow appears during the blade flatting procedure, which results in a redistribution in thickness of the blank. Regions with complex initial shape present considerable thickness changes, while the thickness remains nearly unchanged in other regions where initial curvatures are smooth.

2) After twisting, the distribution of strain is non-uniform due to the structure character. The root can hardly be deformed by twisting. Some grooves appear on the skin due to the biaxial compressive stress state.

3) The mold pressing and inflation adjusting step are proved to be very effective in correcting the blade profile and repairing the skin deflections. Hollow blade with precise configuration can be obtained successfully. The distortion of ribbons can be controlled within a small range with a skin thickness change less than 7.6%.

References

1 Li S F, Zhang D H, Bu K. *Rare Metal Materials and Engineering*[J], 2012, 41(3): 559
2 Xun Y W, Tan M J. *Journal of Materials Processing Technology*[J], 2000, 99(1-3): 80
3 Han Wenbo, Zhang Kaifeng, Wang Guofeng. *Journal of Materials Processing Technology*[J], 2007, 183(2-3): 450
4 Du Zhihao, Jiang Shaosong, Zhang Kaifeng *et al*. *Materials & Design*[J], 2016, 104: 242
5 Huang A, Lowe A, Cardew-Hall M J. *Journal of Materials Processing Technology*, 2001, 112(1): 136
6 Zhang K F, Wang G F, Wu D Z *et al*. *Journal of Materials Processing Technology*[J], 2004, 151(1-3): 54
7 Yoon J H, Lee H S, Yi Y M. *Journal of Materials Processing Technology*[J], 2008, 201(1-3): 68
8 Zhao B, Li Z Q, Hou H L *et al*. *Rare Metal Materials and Engineering* [J], 2010, 39(6): 963
9 Lee C H, Huh H. *Journal of Materials Processing Technology*[J], 1998, 80-81: 76
10 Parsa M H, Matin P H, Mashhadi M M. *Journal of Materials Processing Technology*[J], 2004, 145(1): 21
11 Feng Zhengkun, Champliauda Henri, Sabourinb Michel *et al*. *Simulation Modelling Practice and Theory*[J], 2013, 36: 11

复杂结构的钛合金宽弦空心风扇叶片的双层制造工艺及其毛坯优化设计

陈明和，吴心晨，谢兰生，王　宁，苏　楠
(南京航空航天大学，江苏 南京 210016)

摘　要：钛合金宽弦空心风扇叶片是航空发动机的重要部件，具有复杂的结构特点，内部交替排列减重空腔与加强筋，采用基于复杂超塑性成形的传统多层工艺成形难度大。针对以上问题，提出一种基于热成形和扩散连接技术的新双层制造工艺，并且规划了一条毛坯优化设计的基本技术途径，更可靠可控的构建了内部加强筋。借用 ABAQUS 软件数值模拟成形，分析成形结果的厚度均匀性、结构完整性和表面缺陷，以及评估方法的实用性。以 Ti-6Al-4V 为成形材料，采用经尺寸优化后的最佳坯料，进行了一系列的实验来验证仿真结果。实验成功制造出无缺陷的缩比版钛合金宽弦空心风扇叶片，同时实验与仿真模拟结果非常吻合。

关键词：宽弦空心叶片；毛坯优化设计；扩散连接；有限元仿真；钛合金

作者简介：陈明和，男，1962 年生，教授，南京航空航天大学机电学院，江苏 南京 210016，E-mail: meemhchen@nuaa.edu.cn